Chapter VI

Interaction of tyrosine analogues with quaternary ammonium head group at micelle/water interface and their influence on aggregation characteristics of cationic micelles

1. Introduction

Most cellular membranes are complex assemblies of different lipids and proteins in which phospholipids are the major building blocks. Phosphatidylcholine (lecithin) is usually the most abundant phospholipid in animals and plants. It is a neutral or zwitterionic phospholipid (with quaternary ammonium cation and phosphate anion) over a range of pH. Membranes are thin, fluidic and highly flexible in nature with low bending modulus and permits selective passage of materials from and into the cells as well as allow lateral flow of membrane components in itself.[1] A number of different types of proteins also form an integral part of the cell membrane. These functional protein molecules are bound to the cell membrane through different mechanism and perform various tasks. Some of these crucial proteins are either *transmembrane proteins* which extend across the lipid bilayer or intercellular *anchored proteins* that do not span the membrane but are covalently attached to the inner surface by fatty acids or phospholipids. *Peripheral proteins* are weakly bound to the membrane surface by non-covalent interactions with other membrane proteins but most of the proteins of the plasma membrane that are exposed to cell surface are covalently linked to some sugar molecules.[2-5] The transmembrane proteins, viz., α-helical bundles and β-barrel proteins, localize aromatic aminoacids (especially, tyrosine, tryptophan and histidine) at the membrane/water interface where they form functionally significant H-bonds with interfacial water. The prevalent understanding is that these residues help the anchoring of membrane proteins to the biological membranes via interaction with the lipid head groups. In membrane proteins, these residues have been demonstrated to orient themselves to face the lipid head groups and are part of the so called 'aromatic belt'.[6-9] A highly significant non-covalent interaction, which is believed to occur abundantly in biological systems is cation-π interactions, the weak attractive interactions that exist between cationic species and π-electron cloud of aromatic ring.[10-13] However, the relevance of this interaction in biological structures has been recognized only in recent

years. While the majority of x-ray crystal structure analysis reveals cation-π interaction as one of the main forces that stabilizes protein folding and protein complexes with small molecules, most of the above findings are the results achieved through indirect experiments. Therefore, investigation aimed at individual interactions by other lead techniques are of extreme importance for better understanding of the forces in complex biological organizations.[14-16] Furthermore, neurotransmitters transmit signals across a chemical synapse from one neuron (nerve cell) to another target neuron where the synapse binds specific receptor in the membrane. It is understood that almost all the neurotransmitters contain a cationic center and a common strategy for biological recognition of cation is the cation-π interaction. The nicotinic acetylcholine receptor is the example of ligand-gated ion channel.[17,18] A number of aromatic aminoacids have been identified as contributing to the agonist binding site, suggesting that cation-π interaction is involved in binding the quaternary amino group of the agonist, acetylcholine. Therefore, it is imperative to say that studies on the interaction of aromatic aminoacids with such cationic species as quaternary ammonium group at the membrane/water interface is of particular importance. But, surprisingly, report of such a fundamental study is lacking in the literature. In view of the inherent complexity of the biomembrane systems, use of suitable models for the aromatic aminoacid residues of such proteins would indeed be helpful. In spite of the importance, very few model systems have been developed that could help understand the behavior of aromatic aminoacids viz., tyrosine and tryptophan residues in the membrane. Tyrosine and tryptophan octyl esters are recognized as the important models for the membrane bound aromatic residues.[19-24] It is interesting to note that fluorescence properties of long chain esters of tryptophan (L-Tryptophanoctyl ester), incorporated in model membrane of surfactant micelles, have been shown to be similar to that of tryptophan residue of transmembrane proteins. In the previous chapter, it has been shown that occurrence of hydrophilic and hydrophobic blocks in octyl and dodecyl esters of tyrosine as well as in octyl ester of tryptophan, leads to molecular bending of these aromatic systems in aqueous solutions and eventually fascinating high order morphology of the exclusive aggregates are formed.[25] These self-assembled systems also exhibit high promise toward application as bio-inspired drug carriers.

It will be interesting to pay attention as well, in this context, to the shape of biological membrane and the mechanism of its tuning in various vital processes like cell fusion

and fission. Biological membranes exhibit various function-related shapes, and the mechanism by which these shapes are created is largely unclear. It is generally believed that the changes of membrane topology is produced as a result of a complex interplay between membrane proteins, lipids and certain physical forces. Therefore, it is also tempting to explore whether the aromatic amino acid residues of transmembrane proteins can have any role to play in controlling shape transition of the membranes near head group of phosphatidylcholine.

2. Materials and Methods

2.1. Materials

L-Tyrosineoctyl ester (TYOE) and L-Tyrosine dodecyl ester (TYDE) were synthesized in our laboratory following the procedure published previously.[3] CTAB was purchased from Fluka (Switzerland). D_2O for NMR study was purchased from Aldrich (USA). Purity of all the chemicals were greater than 99.5% and were used as received. All experiments were done with de-ionised and doubly distilled water with pH 6.5-7 and specific conductance below $2\mu S.cm^{-1}$.

2.2. Methods

2.2.1. Tensiometry. Tensiometric measurements were performed on Krùss K9 Tensiometer (Germany), based on Du-Nóuy ring detachment method, fitted with Omniiset temperature bath with precision ± 0.1^0C. Before each measurement, the platinum ring was thoroughly cleaned with 1:1 acetone-water solution and heated under oxidizing flame until glowing temperature was attained. After every addition, the experimental solution was stirred for 5 minutes for homogeneity and equilibrated for 10 minutes. For each measurement, three to five subsequent readings were taken for concordance. Standard deviation was < 0.1 $mN.m^{-1}$.

2.2.2. pH measurements. The pH of the solutions were measured using Systronics digital pH meter (Model: 335, India), calibrated with standard buffers of pH 4.0 and 9.2. Solutions were equilibrated for 5 min after addition of acid/alkali till a steady pH meter reading was observed.

2.2.3. UV-Vis Spectroscopy. UV-Vis study was carried on Jasco V 530 Spectrophotometer fitted with a tungsten filament. A matched pair of glass cuvette of

optical length 1 cm was used for control and sample solutions. The solutions were allowed to equilibrate for 10 minutes before each measurement.

2.2.4. Fluorescence spectroscopy. Steady state fluorescence emission study was carried out in bench top spectrofluorimeter from Photon Technologies International (Quantamaster-40, USA) with excitation and emission slit widths fixed at 3.0 nm and 2.5 nm respectively. Steady state anisotropy (r) was determined using the following expressions[26]

$$r = \frac{I_{VV} - GI_{VH}}{I_{VV} + 2GI_{VH}} \text{ and } G = I_{HH}/I_{HV} \quad \text{(i)}$$

where I_{VV} and I_{VH} represent the intensities obtained with the excitation polarizer oriented vertically and the emission polarizer oriented vertically and horizontally respectively; I_{HV} and I_{HH} refer to the similar parameters as mentioned above for the horizontal positions of the excitation polarizer. The anisotropy values were averaged over an integration time of 60 seconds. Samples were taken in Hellma quartz cuvette of optical length 1.0 cm.

2.2.5. Nuclear Magnetic Resonance Spectroscopy (NMR). ^{1}H NMR experiments were performed in Bruker (Germany) ADVANCE spectrometer operating at 400 MHz. Signals are quoted as δ values in ppm using residual protonated solvent signals as internal standard (D_2O: δ 4.79 ppm). Respective solutions were made in D_2O and 0.6 mL of the same was used for each measurement. Data are reported as chemical shift. 2D Nuclear Overhauser effect spectroscopy (NOESY) spectra was studied using Brucker standard software acquisition program noesyphpr in phase-sensitive mode using 5 mm BBO probe. An acquisition time of 0.085 sec and relaxation delay of 2 sec was used between the scans. The mixing time was 300 milisec. A total number of 2048 complex point were collected. Number of 16 scans were undertaken.

2.2.6. Small Angle Neutron Scattering (SANS). The SANS measurements were carried out using small angle neutron scattering diffractometer at the Dhruva reactor, Bhabha Atomic Research Centre, Trombay, India. The diffractometer uses a beryllium oxide filtered beam with a mean wavelength (λ) of 5.2 Å. The angular distribution of the scattered neutrons is recorded using a one-dimensional (1D) position-sensitive detector (PSD). The accessible wave vector transfer ($Q = 4\pi \sin\theta/\lambda$, where 2θ is the scattering angle) range of the diffractometer is 0.017-0.35 Å^{-1}. The PSD allows

simultaneous recording of data over the full Q. The samples were held in a quartz sample holder of 0.5 cm thickness. The measured SANS data have been corrected and normalized to absolute unit (as cross-section per unit volume), using standard procedures.

2.2.7. Cryogenic Transmission Electron Microscopy (Cryo-TEM). Samples for Cryo-TEM were prepared in controlled environment vitrification system (CEVS). A drop of sample solution was added to 300 mesh copper support grid coated with carbon film. Excess sample was blotted carefully. For vitrification, the TEM grids were plunged rapidly in liquid ethane at -183^{0}C, and stored in liquid nitrogen. The Cryo-TEM images were obtained with Hitachi H-7650 microscope (Japan) operating at accelerating voltage of 120 kV.

2.2.8. Rheology. The rheological experiments were done using cone-plate geometry with 4^0 truncation angle, with diameter 25 mm and sample gap of 0.105 mm sample gap in MCR 302 rheometer (Anton Paar, Germany) equipped with Peltier temperature control system. The samples were initially stirred at 60^{0}C for three hours for homogenization and equilibrated for 72 hrs. During measurement, samples were equilibrated for 10 mins at each temperature.[27]

2.3. Analysis of SANS data

For a system of monodispersed interacting particles, the differential scattering cross-section per unit volume ($d\Sigma/d\Omega$) may be expressed as a function of scattering vector Q as:

$$\frac{d\Sigma}{d\Omega} = n\,(\rho_m - \rho_s)^2\, V^2\, [\langle F(Q)^2\rangle + \langle F(Q)\rangle^2 (S(Q)-1)] + B \qquad (1)$$

where n is the number density of micelles, ρ_m and ρ_s are the scattering length densities of the micelle and the solvent, respectively, and V is the volume of the micelle. F(Q) denotes the single-particle form factor which is the characteristic of specific size and the shape of the scatterer, and S(Q) denotes the interparticle structure factor. B is a constant, which represents the incoherent scattering background. The F(Q) is calculated by treating the micelles as prolate ellipsoids, using the equations:[28]

$$\langle F(q)^2\rangle = \int_0^1 [F(q,\mu)]^2\, d\mu \qquad (2)$$

$$\langle F(q)\rangle^2 = \int_0^1 [F(q,\mu)\, d\mu]^2 \quad (3)$$

$$F(q,\mu) = \frac{3(\sin x - x\cos x)}{x^3} \quad (4)$$

$$x = q[a^2\mu^2 + b^2(1-\mu^2)} \quad (5)$$

where a and b are the semimajor and semiminor axes of an ellipsoidal micelle, respectively, and μ is the cosine of the angle between the directions of a and the wave vector transfer Q. The interparticle structure factor S(Q) identifies the correlation between the centers of different micelles, and it is the Fourier transform of the radial distribution function g(r) for the mass centers of the micelle. S(Q) is calculated using expressions derived by Hayter and Penfold from the Ornstein-Zernike equation and using the rescaled mean spherical approximation.[29] To simplify the calculation of S(Q), the micelle is assumed to be a rigid equivalent sphere of radius $\sigma = (ab^2)^{1/3}$ interacting through a screened Coulomb potential.

3. Results and Discussion

3.1. Surface properties of CTAB-TYOE/TYDE mixtures

The cac and other physico-chemical properties of TYOE and TYDE are reported in Chapter V.[25] In the present chapter, the surface and other related properties of TYOE and TYDE, in presence of CTAB is examined. On the one hand, the cmc values of CTAB decrease significantly as a function of TYOE or TYDE concentrations and the system display significant improvement of surface and bulk properties. On the other hand, the values of γ_{cmc} of the system (in the composition regime of x_1= 0 to x_1=1) are much lower than that of pure CTAB (x_1=1) or TYOE/TYDE (x_2=0). The pC_{20} (negative logarithm of surfactant concentration pure required to reduce the surface tension of water by 20 units at the temperature of measurement) values of the mixed systems are found to be much higher than that of CTAB.

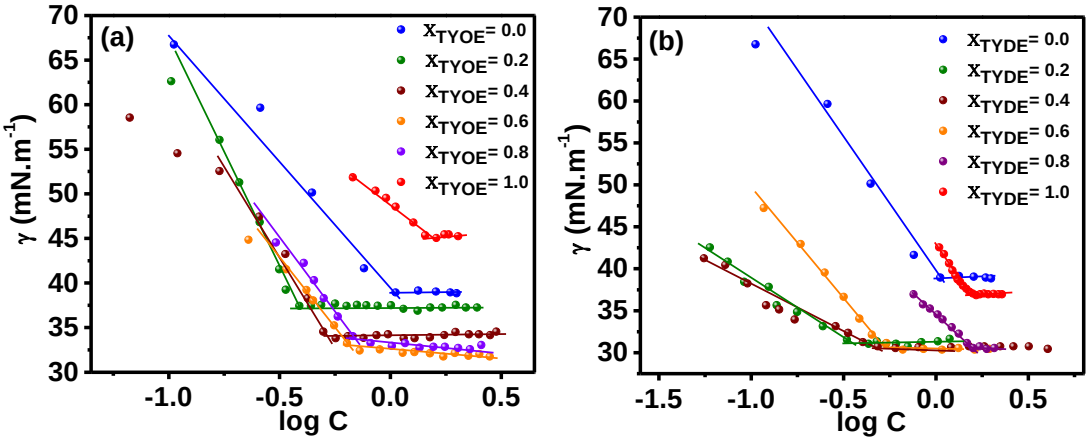

Figure 1. Variation of surface tension of CTAB in presence of (a) TYOE, (b) TYDE, as function of mole fraction at 303 K. C denotes the concentration of CTAB within the mixed systems.

Since the cac value of TYOE (cac = 1.81 mM) and TYDE (cac = 1.31 mM) is much higher than that of CTAB (cmc = 0.9 mM), the cmc of mixed system gives a minima at the aminoacid ester composition of x_1 = 0.2 for both TYOE and TYDE and predictably consistent value of 0.9 mM ($x_{TYOE/TYDE}$ = 0.0) and 1.49 mM (at x_{TYOE} = 1) and 1.45 mM (at x_{TYDE} = 1) for octyl and dodecyl esters of tyrosine respectively. The strong synergism in surface properties as observed at x_{TYOE} and x_{TYDE} of 0.2, is attributed to the electrostatic interaction between the π-electron face of tyrosine ester with quaternary ammonia groups of CTAB. This interaction stabilizes ester-CTAB pairs as the pseudo double tailed surfactant systems, resulting in the stronger hydrophobic interactions in the mixed micelle core and lowers cmc of the system. The CTAB-TYOE/TYDE systems may, therefore, be assumed to behave as mixed surfactant solution.[30] The nature of mixing may be evaluated on basis of Clint's approach. For any mixed component system, the cac is related to individual component as:[31]

$$\frac{1}{cac_{mix}} = \sum_{i=1}^{n} \frac{x_i}{f_{i.}cac_i} \tag{6}$$

where cac_i and cac_{mix} are the cac of the i^{th} component and the mixed surfactant system respectively, x_i and f_i are the mole fractions and activity coefficients of the respective i^{th} component in the mixed aggregate. For ideal mixing, f_i = 1, and Equation 6 may be applied to the present systems as:

$$\frac{1}{cac_{ideal}} = \frac{x_1}{cac_1} + \frac{(1-x_1)}{cac_2} \tag{7}$$

where 1 denotes CTAB and 2 denotes the respective aminoacid esters.

The cac_{ideal} for the mixed systems have been calculated and presented in Table 1. It is evident that the cac of the mixed system deviate significantly from the cac_{ideal}, which reveals that the interaction between the CTAB and the aminoacid ester molecules is non-ideal in nature. The much lower values of cac, along with the tendency of TYOE and TYDE to lower the interfacial tension of CTAB indicates that both TYOE and TYDE molecules synergistically interact with CTAB and modify the aggregation characteristics of CTAB micelles.[32,33] For more insight on the modification of interfacial property of CTAB in presence of TYOE and TYDE, surface parameters viz., equilibrium surface pressure, Π_{cac}, the total surface excess (Γ_{max}^{tot}) and the minimum surface area per molecule (A_{min}^{tot}) of the CTAB-aminoacid ester mixed systems are evaluated (Table 1). Increase in Π_{cac} of CTAB from 32.1 $mN.m^{-1}$,[34] (at $\chi_{TYOE/TYDE} = 0$) to 38.8 $mN.m^{-1}$ at χ_{TYOE} = 0.6 (Table 1) and to 40.9 $mN.m^{-1}$ at χ_{TYDE} = 0.6 indicates enhanced efficiency of surface tension reduction in the mixed surfactant system at these compositions compared to pure CTAB.[35] The A_{min}^{tot}, which is the minimum surface area occupied by a surfactant component at the air-water interface, have been calculated using Gibbs adsorption isotherm (Table 1).[36] The lower A_{min}^{tot} in CTAB-TYOE system, at $\chi_{TYOE=}$0.2 and 0.4, *viz.,* 0.2 and 0.4 nm^2/molecule respectively compared to the individual components, i.e., 0.24 nm^2/molecule for CTAB and 0.49 nm^2/molecule for TYOE, suggest that the mutual repulsion between the surfactant head groups is reduced at these compositions and the components pack closer at the interface.[30] Interestingly, the CTAB-TYDE systems exhibit higher values of A_{min}^{tot} compared to individual surfactants at all compositions (Table 1) indicating much higher hydrophobicity.[35]

3.2. CTAB -TYOE/TYDE interaction

The interaction parameter β, as defined by the regular solution theory, is useful in characterizing the nature and degree of interaction between two nonhomogeneous amphiphile molecules in solution. The β value explains the interaction between the head groups of surfactants. Interestingly, it does not include the interaction between hydrocarbon chains of the amphiphiles when the lengths of the chain are different. The interaction parameter β is determined by measuring cmc of the mixtures of CTAB with aromatic aminoacid esters. The degree of head group interaction in the mixed aggregate systems is measured by calculating β from the equation derived from Rubingh's[37]

theory of non-ideal mixing (Equation 2 in Appendix C). The values of the interaction parameter as determined for the present system is listed in Table 1.

Table 1. Critical aggregation concentration (cac), cac_{ideal}, i.e., cac predicted using Clint's equation; surface parameters viz., equilibrium surface tension (γ_{cac}), surface pressure at cac (Π_{cac}), maximum surface excess concentration (Γ_{max}), minimum surface area per monomer (A_{min}); interaction parameter (β), activity coefficient of CTAB (f_1) and aminoacid esters (f_2) as a function of mole fraction of TYOE and TYDE respectively, in aqueous medium at 303 K

X_{TYOE}	cac_{ideal} (mM)	cac (mM)	γ_{cac} (mN.m^{-1})	Π_{cac} (mN.m-1)	$10^6\ \Gamma_{max}$ (mol.m^{-2})	A_{min} (nm^2 /molecule)	β	f_1	f_2
				TYOE					
0.0	-	0.89	39.1	32.1	6.98	0.24	-	-	-
0.2	0.99	0.36	37.5	33.7	9.08	0.18	-5.26	0.045	0.116
0.4	1.12	0.53	34.1	37.1	8.27	0.20	-3.24	0.126	0.312
0.6	1.28	0.70	32.4	38.8	5.71	0.29	-2.36	0.183	0.515
0.8	1.49	0.72	33.1	38.1	6.09	0.27	-3.01	0.086	0.573
1.0	-	1.81	45.1	26.1	3.38	0.49	-	-	-
X_{TYDE}				TYDE					
0.0	-	0.89	39.1	32.1	6.98	0.24	-	-	-
0.2	0.95	0.38	30.9	40.3	2.54	0.65	-4.47	0.067	0.169
0.4	1.02	0.50	30.4	40.8	2.53	0.65	-2.83	0.147	0.397
0.6	1.10	0.55	30.3	40.9	4.91	0.34	-2.63	0.136	0.532
0.8	1.19	1.29	30.4	40.8	3.55	0.47	-1.71	0.262	0.684
1.0	-	1.31	37.8	33.4	5.29	0.31	-	-	-

A number of interesting features are apparent. The β values for all compositions of binary mixtures are negative, indicating more attractive interaction to exist in the mixed micelles compared to the self-assembly of the individual amphiphile. According to the regular solution theory, the β parameter should be independent of composition. Indeed, the β parameter values in the present study lie within close range of (2.91-2.56) and (2.31-2.09) for CTAB-TYOE and CTAB-TYDE respectively in the composition (x) regimes of x_1 =0.4 - 0.8. At low and high x, the β is more negative due to self-assemblies of the CTAB and aminoacid esters respectively rather than mixed micelle formation. It is also interesting to mention that the average value of β ($x_1 \rightarrow$ 0.4 - 0.8) for CTAB-TYOE and CTAB-TYDE mixtures are found to be -2.72 and -2.35 respectively. This indicates that the interaction between quaternary ammonia head groups of CTAB with aromatic aminoacid esters is stronger in TYOE compared to TYDE, although the TYDE molecules contains longer hydrocarbon chain in its molecular framework. This result is indeed surprising and needs to be examined carefully by means of subsequent experiments.

3.3. UV-Vis absorption and study of micropolarity.

UV-Vis absorption spectra of 0.2 mM aqueous TYOE exhibit a red shift of about 3 nm with $\lambda_{max,}$ varying from 274 nm to 277 nm, upon addition of CTAB (Figure 2). Aromatic compounds, in general, exhibit two strongly overlapped bands in the near UV region, viz., longitudinally polarized $^1L_a \leftarrow {}^1A$ and the transversely polarized $^1L_b \leftarrow {}^1A$ band.[38] Distinct isobestic points at 297 nm, 270 nm and 246 nm are observed in the spectra for sub micellar concentration regime, indicating that the interaction between the aromatic aminoacid and the quaternary ammonium ion head groups to occur even at the water/air interface, prior to self-assembly formation of CTAB in aqueous solution. The absorbance-concentration profile at the $\lambda_{max,}$ exhibits linear variation with a break point close to cmc. This shows that the interaction of amino acid esters with CTAB molecules is fairly strong and the aromatic esters are embedded rather strongly once the micelles of CTAB are formed above the cmc. The energy associated with this apparently small shift in the λ_{max} is found to be nearly 1.13 kcal.mol^{-1}. It is interesting to note that in a theoretical study, the energy involved in cation-π interaction in solvent separated quaternary ammonia-benzene system in aqueous media has been shown to be 1.67 kcal.mol^{-1}. The folded molecular geometry of TYOE molecules are probably embedded in the CTAB micelles with the hydrophilic block consisting of ethereal oxygen, amine

and carbonyls groups protruded toward the interfacial water and the aromatic face of TYOE molecule is arranged near the quaternary ammonium head group. Presence of isobestic points, both in pre and post micellar regions (shown in Figure 3) indicates that interaction between CTAB headgroups and aromatic moieties of esters takes place at the solution interface (pre micellar regime) as well as in the bulk (post micellar regime).

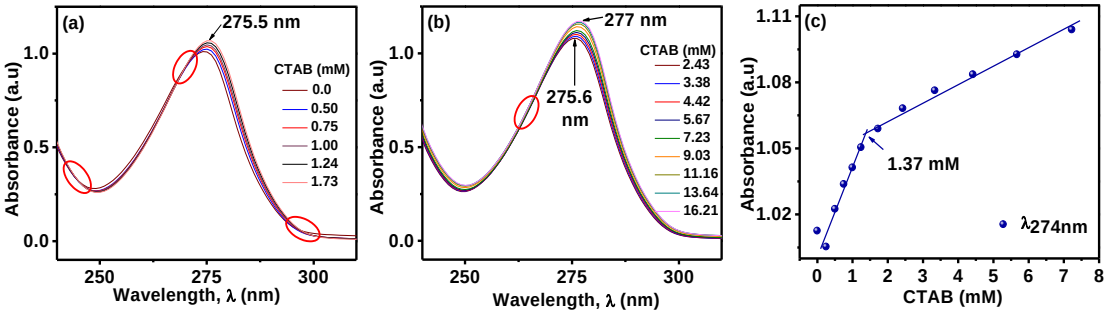

Figure 2 (a) Effect of addition of CTAB in the pre-micellar regime on absorption spectra of 0.2 mM aqueous TYOE at 303 K, (b) Effect of addition of CTAB in the post-micellar regime on absorption spectra of 0.2 mM aqueous TYOE at 303 K, (c) Variation of absorption intensity of 0.2 mM TYOE at 274 nm with CTAB concentration at 303 K.

In the case of 0.2 mM TYDE, the intensity at absorption at λ_{max} 277 nm (initially decreases (upto 1.27 mM which is slightly above the cmc of CTAB, i.e. 0.9 mM) (Figure 3 (a)) and increases thereafter (Figure 3 (b)) in the post-micellar region. An isobestic point is observed at 265 nm. A red shift of 1 nm was observed in the post-micellar region, where absorption maxima varies from 277 nm to 278 nm.

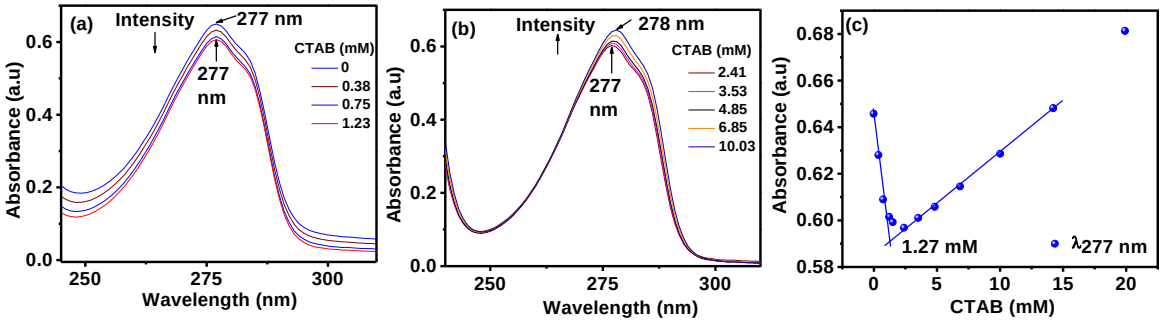

Figure 3 (a, b) Effect of addition of CTAB on absorption spectra of 0.2 mM aqueous TYDE at 303 K, (c) Variation of absorption intensity of 0.2 mM TYDE at 274 nm and 276 nm with CTAB concentration at 303 K.

The contrasting result may originate from the rigidity of folded geometry of TYDE molecule, the aromatic group of which flips upward due to a slight obliquely tilted alkyl

chain inside the micelle core via stronger force of hydrophobic interactions. As a result, the phenol group of TYDE localizes to little deeper in bulk water, diminishing the interaction with the head group.

An important aspect of tyrosine is its pH dependent dissociation of the phenolic OH proton in aqueous solution. Study of the micropolarity of the charged interface could also provide a better understanding of the exact nature of the location of the OH groups at the vicinity of CTAB micelles. Any changes in surface potential and polarity at the charged interface would be reflected in the acid-base equilibrium of the dissociation of the hydroxyl protons.[39,40] Therefore, determination of the pKa values and its changes could provide vital information about the underlying interaction phenomenon occurring within the CTAB-aminoacid ester systems. Assuming the dissociation of the hydroxyl proton of the tyrosine moiety as:[41]

$$R - OH + H_2O = RO^- + H_3O^+$$

where $R - OH$, RO^-, H_3O^+ are the deprotonated, protonated (neutral) form of the phenolic OH group of the aminoacid esters, viz., TYOE and TYDE, and the hydrated proton respectively. Change in UV spectra as a function of bulk aqueous pH provide the apparent pKa values using Handerson-Hanselbach equation-

$$pK_a = pH - log[\frac{RO^-}{ROH}] \quad (8)$$

The quantity $[\frac{RO^-}{ROH}]$ is determined as $\frac{[A-A_{ROH}]}{A_{OH^--A}}$ where *A*, A_{ROH}, A_{OH^-} are absorbances of the aminoacid esters at experimental, low and high pH's respectively. The pK_a^{obs} may be separated into electrostatic and non-electrostatic components respectively as follows:

$$pK_a^{obs} = pK_a^0 - \frac{e.\psi_0}{2.303kT} \quad (9)$$

where pK_a^0 is the apparent pK_a^{obs} in absence of any surface potential i.e., at . ψ_0 = zero. Comparing the pK_a^0 values of the aminoacid esters in aqueous CTAB micellar media to the pK_a in aqueous-organic mixtures viz., 1,4-Dioxane – water mixtures, will provide the necessary information about the acid-base equilibria at the micellar interface. Defining apparent pK_a in aqueous-organic solvent mixtures, pK_a^m, as:

$$pK_a^m = B + logU_H^0 - \log\left[\frac{RO^-}{ROH}\right] - \log\left[\frac{\gamma_{OH^-}^m}{\gamma_{ROH}^m}\right] \quad (10)$$

where γ^m term denotes the respective activity coefficients, B is the pH meter reading and $logU_H^0$ is the associated correction factor. The pK_a^0 values relate to an interfacial phenomenon whereas the pH measured is that of the bulk solution. Therefore, while comparing between the pK_a in 1,4-Dioxane-water mixture and pK_a^0 in the micellar systems, the primary medium effect on the proton, ${}_m\gamma_{H^+}$, needs to be considered, i.e., pK_a^0 should be compared with pK_a^i rather than pK_a^m, where i stand for interface. These are related as:

$$pK_a^i = pK_a^m + {}_m\gamma_{H^+} \quad (11)$$

Usually, the mean primary medium effect on HCl, ${}_m\gamma_{\pm}$ approximately gives ${}_m\gamma_{H^+}$. The values of ${}_m\gamma_{\pm}$ and U_H^0 are adopted from works of Drummond and co-workers.[39,40] In determining the pK_a^0 values for aminoacid esters in the CTAB micelles, a surface potential of ±141mV is assigned to CTAB.[40] Comparing ΔpK_a^0 of micellar surface and ΔpK_a^i in 1,4-dioxane-water mixtures, the effective dielectric constant, D_{eff} , of the medium at the location of the dissociable proton is found out. The evaluation of the effective dielectric constant considers the underlying assumptions are- (i) both the protonated and the deprotonated forms of the aminoacid esters are quantitatively partitioned within the micellar phase at high CTAB-aminoacid ester ratio, and (ii) since the concentration of the aminoacid esters is low, the activity coefficients terms $\frac{\gamma_{OH^-}^m}{\gamma_{ROH}^m}$ can be neglected such that ΔpK_a^0 can be compared to ΔpK_a^i in different solvent media. The results of pH metric titrations are summarized in Table 2. (UV Absorptions plots as function of pH are provided in Figure S1of SI). The pK_a^w of the phenolic –OH of the tyrosinate moiety in TYOE and TYDE in aqueous media at 298 K was found to be 9.05 and 9.25 respectively for TYOE and TYDE which is close to that of L-Tyrosine in aqueous media (pK_a^w 9.35).[42] The D_{eff} decreases only very slightly on increasing CTAB concentration from 50 mM to 100 mM. Previous study based on solvatochromic visible absorption maxima on CTAB micelles show that the D_{eff} at the micellar interface is around 28-33. In a similar study of CTAB micelles, the D_{eff} in presence of 1 Naphthol was found to vary within 49-51 for 50 mM and 100 mM CTAB.[43] It was concluded that the hydroxy group of 1 Naphthol were directed away from the micellar

surface and resided at a more polar environment. Present study shows that the D_{eff} for TYOE ranges within 40.8 to 40.2 while that for TYDE ranges from 56.9 to 57.9 for 50 mM and 100 mM CTAB respectively (Table 2) which is much higher than that at the CTAB micellar interface. Therefore, it may be said that both TYOE and TYDE locate in such a manner that their OH groups are directed away from the micellar interface, and towards the bulk of the aqueous solvent which is highly polar (D_e of water = 78). Moreover, compared to TYOE, the phenolic OH in TYDE reside further away from CTAB micellar interface, while the phenolic ring of TYOE is located relatively nearer to the CTAB micelles. One of the reasons behind this orientation may be the higher hydrophobic character of TYDE compared to TYOE due to its longer hydrophobic alkyl chain. Nevertheless, this study explains the less interaction of the TYDE molecules with CTAB micelles as observed from SANS study (discussed later).

Table 2: Results of pH titration of 0.2mM TYOE and 0.2 mM TYDE in aqueous solution and aqueous CTAB solutions at 298 K.

CTAB Concentration (mM)	pK_a^w	pK_a^{obs}	ΔpK_a^{obs}	pK_a^0	ΔpK_a^0	D_{eff}
			TYOE			
50 mM	9.055	9.82	2.12	12.20	4.5	40.8
100 mM		10.02	2.31	12.34	4.69	40.2
			TYDE			
50 mM	9.25	10.08	4.6	12.46	3.21	57.9
100 mM		10.53	5.05	12.91	3.66	56.9

3.4. Fluorescence depolarization and steady state emission study.

The degree of depolarization of fluorescence emission of a fluorophore is an index of rotational diffusion during the lifetime of its excited state. Any alterations in microstructure of fluorophore is reflected in the micro viscosity of the probes and hence in their anisotropy values. Therefore this technique is widely employed in exploring the structural modifications of micro heterogeneous systems.[44] As the tyrosine moiety in TYOE and TYDE, are fluorescent active species,[42] fluorescence steady state anisotropy study was done to gain further insight on change in microenvironment of the TYOE and TYDE molecules in presence of the CTAB micelles. Figure 4 shows the variation

of fluorescence anisotropy of 5μM aqueous TYOE and TYDE solutions as function of CTAB concentration at 303 K.

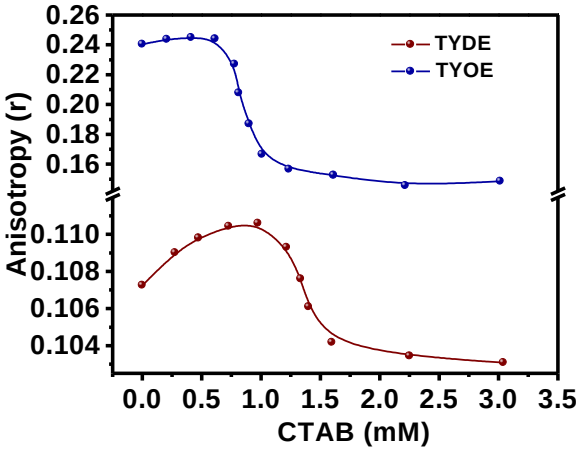

Figure 4. Variation of steady state fluorescence anisotropy of 5 μM aqueous TYOE and 5 μM aqueous TYDE as function of CTAB concentration at 303 K.

It is evident that, the initial anisotropy value (r_0) of TYDE in aqueous solution i.e., 0.24, is much higher compared to TYOE i.e., 0.11. Higher r_0 value imply greater rotational restriction experienced by TYDE in solution. This may arise due to tighter packing of the longer alkyl chains in TYDE compared to TYOE. Figure 4 shows that on increasing CTAB concentration, the anisotropy increases up to a certain point after which, the value diminishes progressively. This critical concentration limit is found to be 1.01 mM in TYOE and 0.66 mM, in TYDE. In both the cases, it corresponds to a concentration near to the cmc of CTAB (0.89 mM). This shows that the aminoacid ester molecules, which act as fluorescent probes, bind with the CTAB monomers till micellization occurs. The cationic micelles consist of a nearly water-free hydrophobic micellar core with polar head groups forming the palisade layer. As CTAB is present in large excess (probe: CTAB~1:120, at cmc) it may be assumed that at cmc, all the probe molecules are bound to the CTAB micelles. Further addition of CTAB increases the number of micelles in solution. The constant population of probes is therefore now redistributed within the enhanced number of micelles and hence we observe the decrease in anisotropy values. The fluorescence emission spectra of 5 μM TYOE and 5 μM TYDE in presence of the CTAB micelles are shown in Figure 5. Upon excitation at the wavelength of maximum absorption, the neutral form of tyrosine emits near 303 nm while the tyrosinate form emits near 340 nm.[42] The emission intensity increases on addition of the CTAB in both TYOE and TYDE (Figure 5 (a), (b)). Insets show that

there exists a break in the intensity vs concentration plots, at 1.05 mM in TYOE and at 0.99 mM in TYDE, which corresponds to the respective cmc of CTAB. This observation corroborates the trend observed in anisotropic behavior of the aminoacid esters. The relative intensities of the neutral (I_N) and tyrosinate (I_T) form depend upon the surrounding medium i.e., in presence of proton acceptor, the tyrosinate band is expected to predominate whereas the neutral form will dominate when no proton acceptor is present in the immediate vicinity.[42]

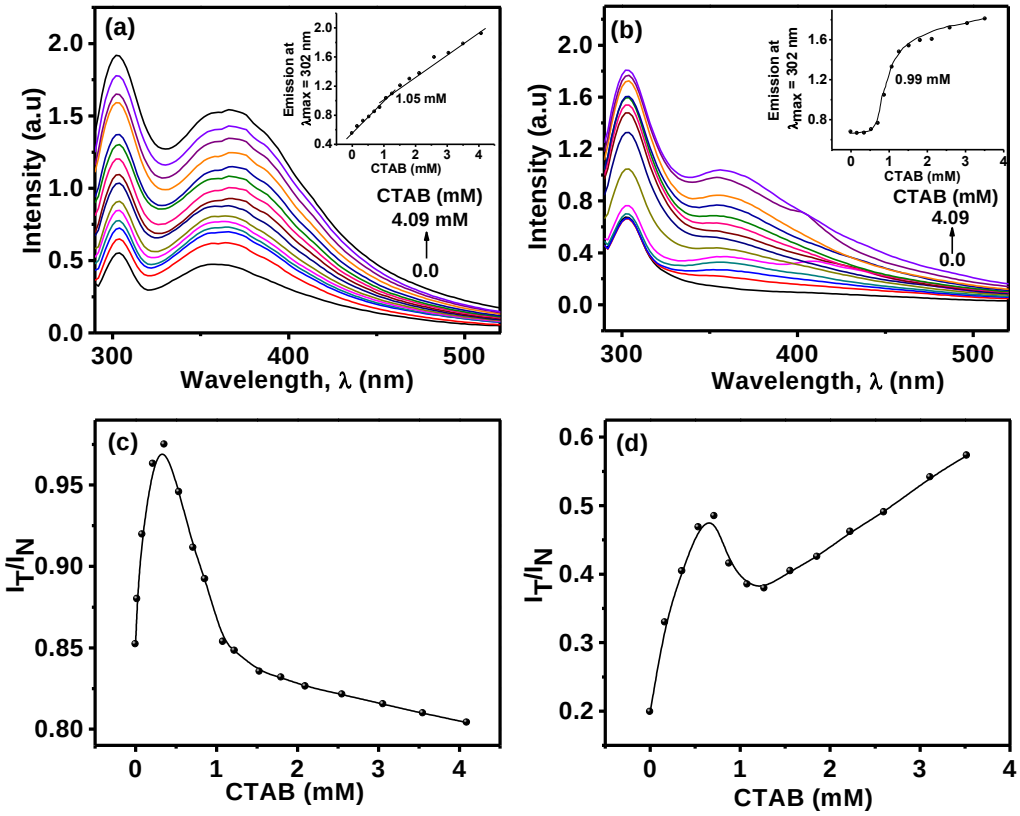

Figure 5. Modification of steady state fluorescence emission spectra of (a) 5µM aqueous TYOE (b) 5µM aqueous TYDE, as function of CTAB concentration at 303 K. Insets display emission at λ_{max} (neutral) as function of respective concentration, Plots of ratio of anionic (I_T i.e tyrosinate emission) to neutral (I_N) emission or, (I_T/I_N) as function of CTAB concentration of (c) 5µM aqueous TYOE and (d) 5µM aqueous TYDE, at 303 K.

Greater inherent positive charge imply higher concentration of hydroxyl ions in immediate vicinity which may act as proton acceptor.[45] The initial linear increase in the ratio of I_T/I_N in both TYOE and TYDE show that proton transfer from the phenolic hydroxy group of tyrosine moiety is facilitated as concentration of micelles increase (Figure 5 (c), (d)). The decrease thereafter indicate that the neutral form in present in excess and that the micelles do not act effectively as proton acceptor.

3.5.1. ^{1}H NMR Study

^{1}H NMR Study is an important tool for identifying the time-averaged location of aromatic solubilized species within surfactant micelles, based on the dependence of chemical shifts of protons in surfactant and aromatic units, on the composition of the aqueous phase. In order to investigate on the relative arrangement of the model aminoacid molecules, viz., TYOE and TYDE with the CTAB molecules in the mixed systems, ^{1}H NMR spectra of the mixture were recorded in aqueous medium (D_2O). The molecular structure and proton numbering of CTAB, TYOE and TYDE are given in Scheme 1.

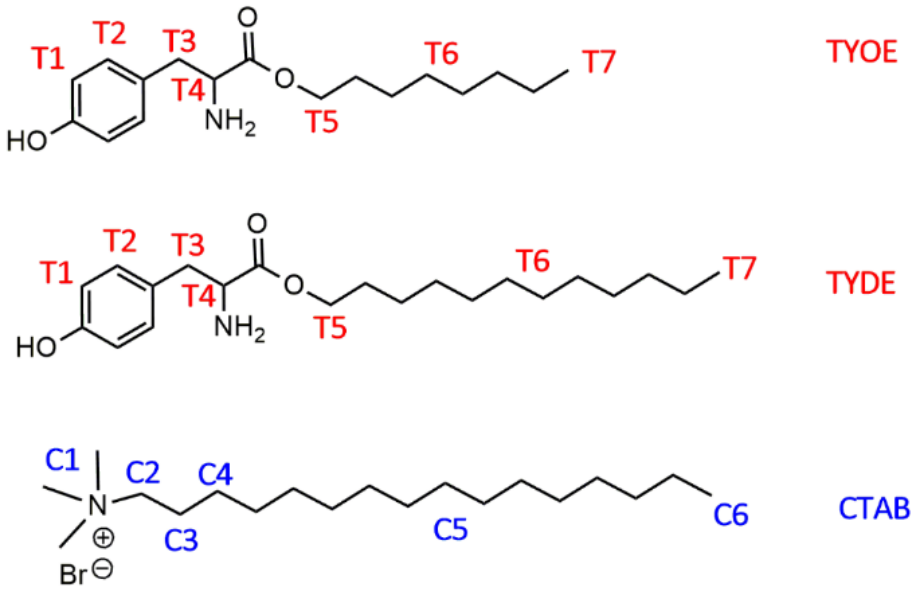

Scheme 1. Schematic presentation of structures and proton numbering of TYOE, TYDE and CTAB.

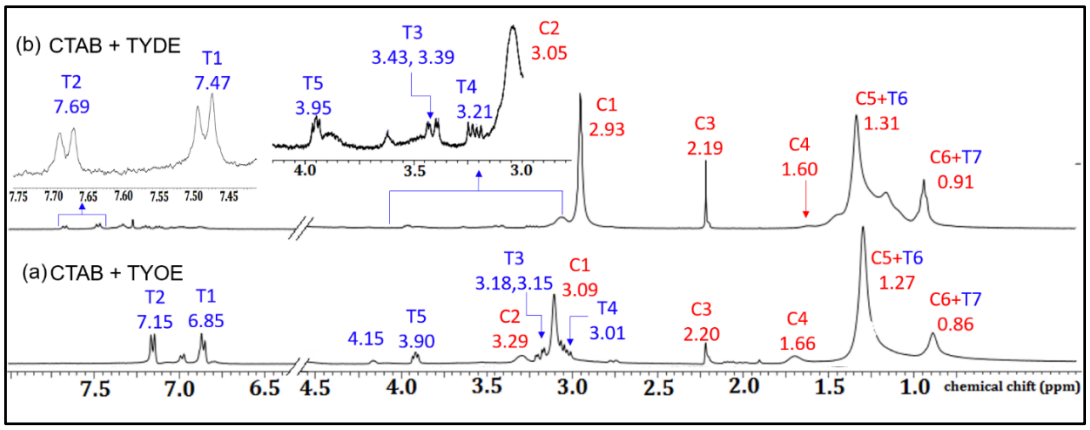

Figure 6. Comparative ^{1}H NMR spectra of (a) CTAB (10 mM)-TYOE (5 mM) and (b) CTAB (10 mM)-TYDE (5 mM) mixed systems in D_2O at 303 K.

The ^{1}H NMR spectra of CTAB (10 mM)-TYOE and CTAB (10 mM)-TYDE (5 mM) mixed systems in D_2O at 303 K is presented in Figure 6. The key resonances are highlighted in the figure. The terminal methyl protons of TYOE resonate at 1.17 ppm in D_2O,[25] whereas, in presence of CTAB, only a single peak at 0.86 ppm corresponding to the resonances of terminal methyl protons of both CTAB (C6) and TYOE (T7) is observed (Figure 6 (a)). This imply that T7 and C6 protons experience similar environment in the CTAB-TYOE mixed system. This shows that the T7 protons of the aromatic amino acid ester experiences considerably more non-polar environment compared to that of which is considerably non polar compared to that of its own self-assembled aggregates. Moreover, in absence of CTAB, the chain protons of TYOE appeared considerably downfield[25] at 3.16 ppm, whereas in presence of CTAB, these signals merged with that of CTAB chain protons and resonates at 1.27 ppm. This further indicates greater hydrophobic environment to exist around the chain protons of TYOE (T6) in presence of CTAB. It has been reported, both experimentally and theoretically, that in aqueous solution, the TYOE moiety prefer folded conformation with the NH_2 and the carbonyl groups oriented toward interfacial water while the aromatic ring and the alky chain are embedded towards the aggregate core.[25,23] 2D NMR analysis of TYOE in aqueous medium further revealed that the alkyl chain of TYOE “bend inwards” due to which the terminal protons of TYOE reside near the aromatic face of the same resulting in a polar environment around the terminal and chain protons of TYOE. Therefore, it may be said that, in presence of CTAB, the orientation of TYOE is modified such that alkyl chain remains in a straight conformation similar to CTAB alkyl chain wherein hydrophobic non polar micro environment is experienced by the alkyl and terminal protons of both the moieties. This conformation of TYOE may be

driven by the mutual strong hydrophobic interactions between the alkyl chain protons of TYOE and CTAB.

Now, let us turn to dodecyl ester of tyrosine, i.e., TYDE. It is evident that the aromatic protons of TYDE in CTAB-TYDE (Figure 6 (b)) system appear relatively downfield compared to TYOE (Figure 6 (a)) which indicates that the T1 and T2 protons of TYDE experience a greater de-shielding of magnetic resonance as compared to the same in TYOE i.e., TYDE aromatic protons reside at more polar environment compared to TYOE. The more polar environment might be due to the interfacial water molecules present around T2 and T1 of TYDE, which is protruded towards the interfacial water, as also indicated from the micro polarity study. Resonance for T3 and T4 protons in CTAB-TYDE system appear significantly downfield compared to CTAB-TYOE suggesting that these protons experience relatively more polar environment like T1 and T2, compared to the same in CTAB-TYOE system. On the other hand, C1 and C2 appear upfield. This observation supports the idea that the CTAB head group are localized near non-polar region, in between the alkyl chains of TYDE monomers. It shows that indeed the TYDE molecule remain "pushed outward" such that the aromatic part is indicates that aromatic part of the TYDE molecules projected out of the micellar interface and remains close to the interfacial water. Consequently, T1, T2, T3 and T4 protons of TYDE molecules are located towards the bulk water and therefore, the signal for T5 proton in CTAB-TYDE system appear at slight downfield compared to CTAB-TYOE system because in the former it remains at the proximity of the CTAB headgroups. The relatively downfield chemical shifts of the intermediate chain protons and the terminal protons in TYDE may be due to the greater spatial distribution of the alkyl chains as result of formation of longer cylindrical micelles.[32, 46]

This observation is rather surprising, because TYDE with longer chain, is expected to be embedded more deep inside CTAB micelles compared to TYOE. However, the similar results is observed in thermodynamic and spectroscopic measurements as well, indicates that it may be connected with folded and rigid geometry of the aromatic esters. It may be argued that as the longer alkyl chain of TYDE experiences stronger hydrophobic interaction with CTAB micelles compared to TYOE, the alkyl chain of the former favors entrenchment deeper inside the CTAB micelle, and due to its rather folded geometry the aromatic moiety flips towards interfacial water, over ridding the

weak attractive force via cation-π interaction at the headgroups. The TYDE molecules are now more tilted obliquely as shown in Scheme 2.

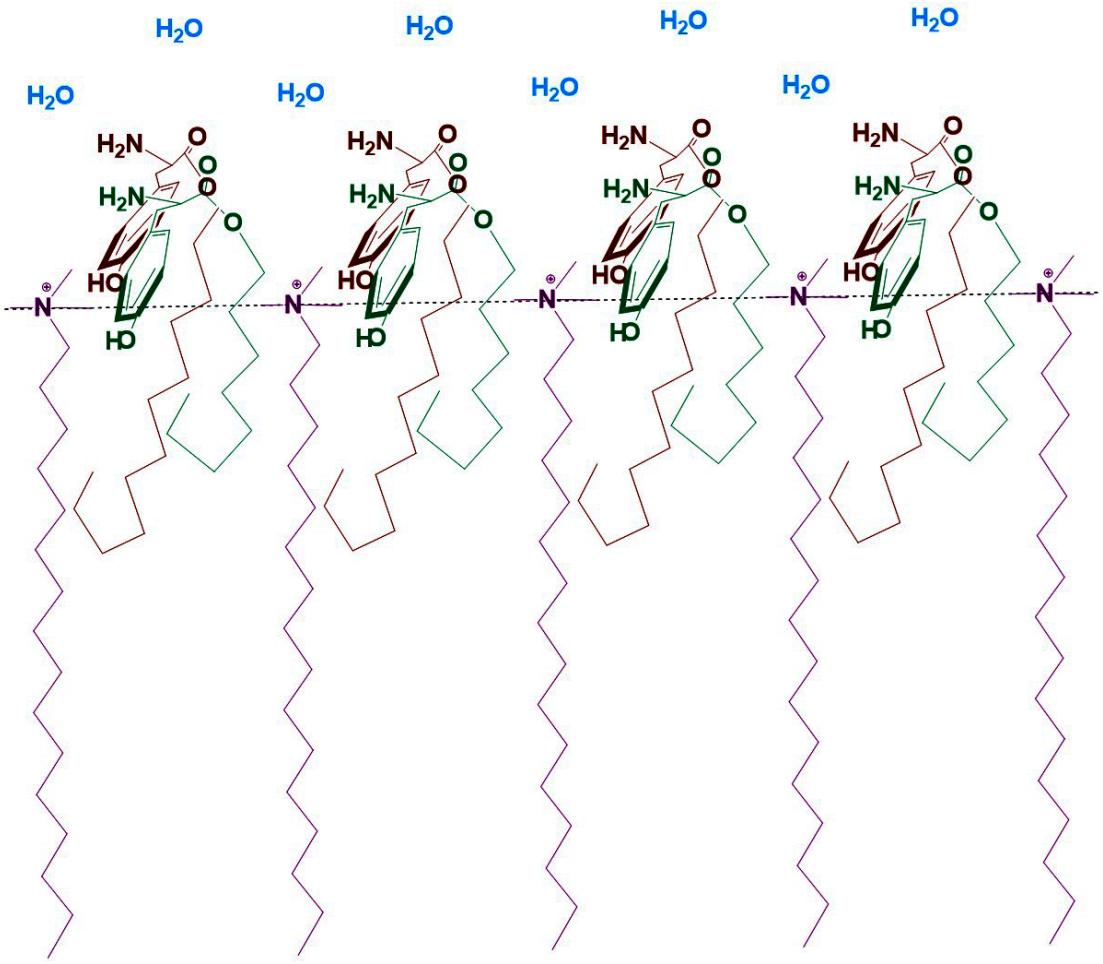

Scheme 2. Possible orientation of TYOE and TYDE w.r.t. CTAB molecules at the micelle/water interface of the wormlike micelles.

3.5.2. NOESY Study

Nuclear Overhauser effect spectroscopy (NOESY) is a 2D NMR technique based on correlation of signals arising via dipolar interaction from the protons that are located close in space (<5Å). The intensity of cross peaks of NOESY spectra is a measure of the extent of magnetization transfer between the proton nuclei and is proportional to the internuclei distance.[47] The NOESY spectra of CTAB (10 mM) and TYOE (5 mM) system, is recorded at 303 K (Figure 7). The intense key cross-peaks, T2-C1 and T1-C1 (Figure 7), correlating the aromatic protons T2 and T1 with the NMe protons of CTAB show that the benzene ring of TYOE is located in the vicinity of the quaternary ammonium head of CTAB (<5 Å). The folded geometry of TYOE favors hydrophilic

blocks consisting of amine, carbonyl and the ethereal oxygen to localize near interfacial water and the aromatic face near quaternary ammonium head groups. This orientation allows an effective cation-π interaction to take place. The key cross-peaks T2-C6+T7, T1-C6+T7 and T2-C5+T6, T1-C5+T6, which are observed in the present system, correlate the aromatic protons with the terminal and the hydrocarbon chain protons, of CTAB and TYOE respectively. Intense cross peak C1-C5+T6, correlating the NMe protons of CTAB with the alkyl chain protons of CTAB as well as TYOE are also observed. These cross peaks are particularly interesting because they suggest that both the aromatic system of TYOE and the quaternary ammonium head group of CTAB are present within the proximity of the chain protons of both CTAB and TYOE. Similar cross peaks were observed in the CTAB (10 mM)-TYDE (5 mM) system as well. Molecular folding is indeed possible in both TYOE and TYDE due to the presence of hydrophobic and hydrophilic blocks in the molecule, such folding is not possible in CTAB molecules. However, keeping in view the transition of morphology from spherical to rod like/wormlike micelles under the present concentration condition of CTAB and TYOE, above spectroscopic observation could be justified if we consider the end-cap region of the rods rather than spherical micelles or body of the rods. A revisit of the geometry of the end-caps is, therefore, necessary to find the explanation of above observation. Further discussion on the geometry of end-caps of rod/worm like micelles is presented in section 3.8 of this report.

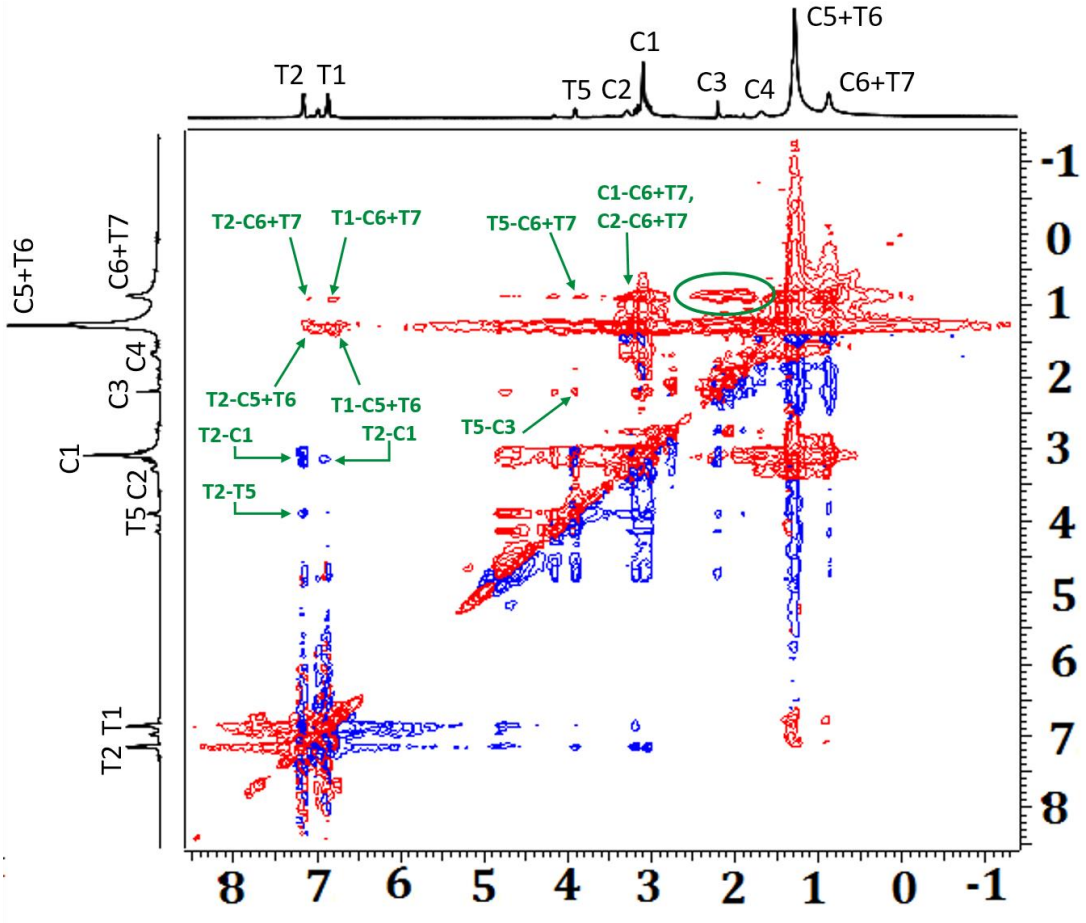

Figure 7. 2D NOESY spectrum of 10mM CTAB and 5mM TYOE in D_2O at 303 K

3.6. Cryo-TEM study

For direct visualization of the CTAB-aminoacid aggregates, Cryo-TEM images of CTAB-TYDE systems were obtained (Figure 8). Figure 8 (a) shows the presence of abundant small spheroidal micelles along with the elongated micelles at 100 mM CTAB and 40 mM TYDE concentration. When concentration was increased to 60 mM, long worm-like micelles developed (Figure 8 (b)). The elongated micelles create a network of entangles thread-like structure due to which the viscosity as well as the elasticity of the system increases. The presence of very few micellar ends implies that the micelles are probably at their longest form.[48] At further higher concentration of TYDE, viz., 75 mM, breakdown of the network occurs and system forms prominent vesicles (Figure 8 (c)). The cryo-TEM images provide inevitable support to the observation of change in micro-structure of CTAB in under the influence of the aminoacid analogues.

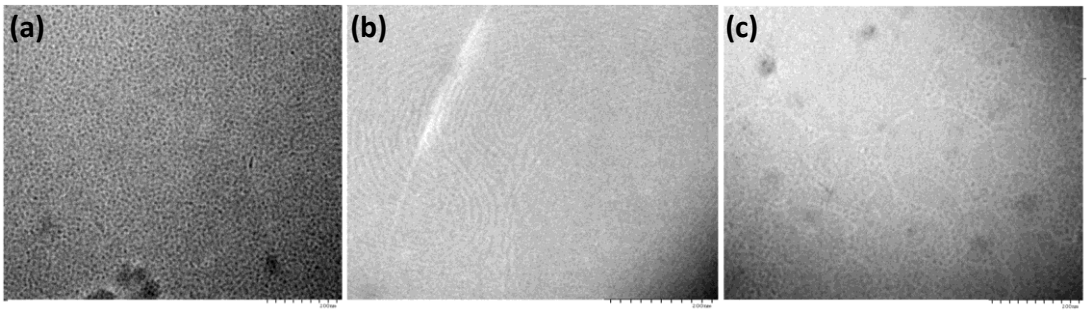

Figure 8. Cryo-TEM micrographs of aggregates of (a) 100 mM CTAB -40 mM TYDE, (b) 100 mM CTAB-60 mM TYOE, and (c) 100 mM CTAB-75 mM TYDE.

3.7. Small angle neutron scattering (SANS) study.

Information regarding structural polymorphism of self-assembled aggregates in solution may be obtained from SANS spectroscopy, in a non-invasive manner.[49] In a SANS experiment, the experimental sample is subjected to a beam of neutrons and the scattered intensities at different directions are measured. As the neutrons are scattered by the nuclei of the atoms, large scattering contrast can be achieved in deuterated solvents compared to protonated solvents as deuterons and protons differ largely in their respective neutron scattering capacities. The microstructural modification of CTAB micelles in presence of the aminoacid ester systems were studied with the help of SANS spectroscopy.

Figure 9 (a) shows the SANS spectra of (100 Mm) CTAB-(40 mM) TYOE and (100 mM) CTAB-(40 mM) TYDE mixed systems at 303 K. Measurements were taken with Q range of 0.017 to 0.358 $Å^{-1}$. SANS distribution for both the CTAB-TYOE and CTAB-TYDE systems display a rise in the low Q region whereas the intensity at high q region is independent of the nature of the aminoacid ester. For CTAB-TYOE system, a broad peak is evident at intermediate Q region, which becomes sharper in the case of CTAB-TYDE system. This peak arises due to the corresponding correlation peak in the interparticle structure factor, S(Q), which generally occurs at $Q \approx \frac{2\pi}{d}$, where d is the average distance between the aggregates present in the sample. Appearance of the correlation peak at nearly identical Q for both CTAB-TYOE and CTAB-TYDE systems suggest that the aggregate density in both the systems is nearly equal.[49] The well-defined and sharp nature of the correlation peak in CTAB-TYDE system indicates that electrostatic repulsion is predominant within the aggregates in this system. The broadening of the correlation peak in the case CTAB-TYOE system imply effectively

reduced interparticle repulsion within the aggregates.[50] A slope of -1 in the low Q region for all the SANS spectra is indictive of the presence of rodlike or elongated aggrregates in the system (Figure 9).[51,52] The experimental data was fitted with the theoretical curves (solid line) obtained on basis on Heyter and Penfold's approach of analysis considering the micelles as prolate ellipsoids.[53] It is evident that this model of micelles fits very well to the experimental data (Figure 9 (a)) confirming the presence of cylindrical or rod-like micellar aggregates within the systems. The increase in intensity of the low Q region in the case of CTAB-TYDE system further indicate growth in micellar size.[54] The observation reveals that the aminoacid esters are efficient in screening the electrostatic repulsive interaction between the quaternary ammonium head groups of the CTAB micelles, which results in one dimensional micellar growth forming elongated micelles.[50,51,55,56]

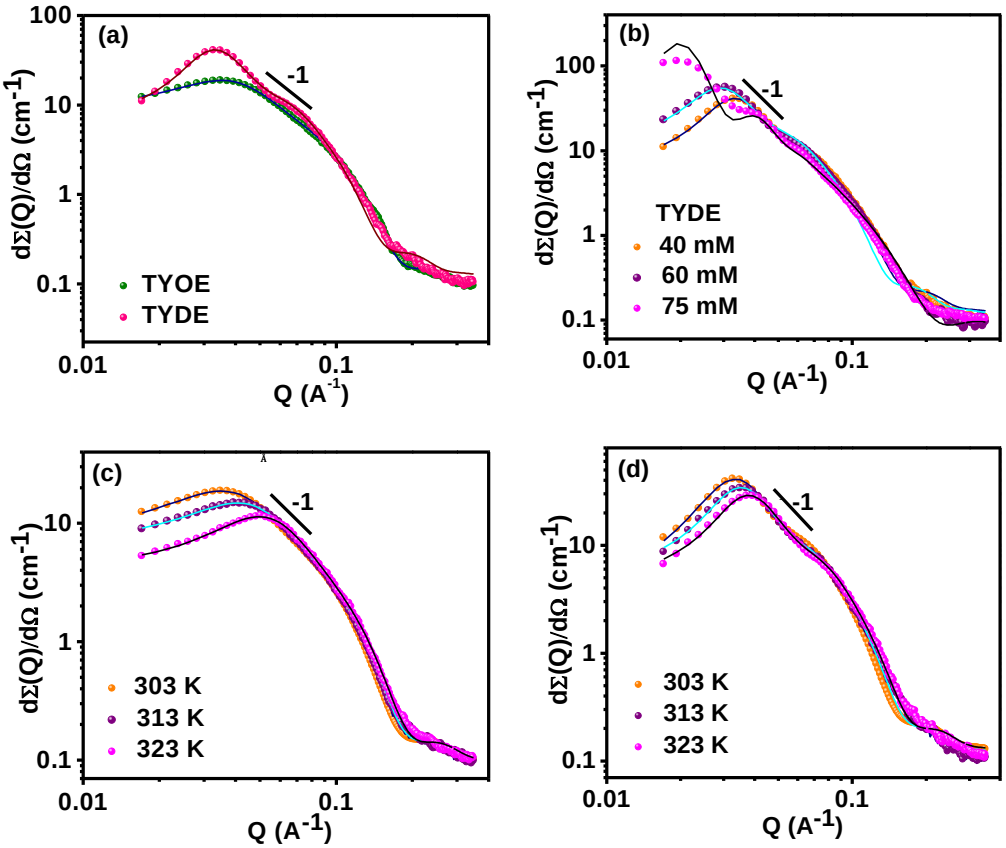

Figure 9. (a) SANS distribution of CTAB (100 mM)-TYOE (40 mM) and CTAB (100 mM)-TYDE (40 mM) systems at 303 K, (b) SANS profile of CTAB (100 mM)-TYDE system as function of TYDE concentration at 303 K, (c) Effect of temperature on CTAB (100 mM)-TYOE (40 mM) system, and (d) Effect of temperature on CTAB (100 mM)-TYDE (40 mM) system. Solid circles represent experimental curve, solid lines represent theoretical fit for prolate ellipsoid micelle model.

This observation is highly significant as it exemplifies the role of the tyrosine analogues, which are abundantly present in transmembrane proteins, in modifying the surface curvature of the lipid membranes which largely consists of phosphocholine derivatives having quaternary ammonium head groups similar to CTAB. SANS study of CTAB-TYDE system as function of TYDE concentration (at constant CTAB concentration of 100 mM) show that longer micelles form at 60 mM TYDE compared to 40 mM concentration as evident from the increase in correlation peak intensity in the SANS profile (Figure 9 (b)). At TYDE concentration of 75 mM, the spectra deviates from the prolate ellipsoidal model fit, implying a major structural change at this composition. The effect of temperature on 100 mM-40 mM CTAB-aminoacid composition is studied (Figure 9 (c), (d)). With rise in temperature, the intensity of the correlation peak increases with shifting of Q_{max} to higher Q values. The shift in Q_{max} suggests a decrease in correlation length, ξ, given by $\xi = 2\pi/Q_{max}$[57] i.e., with rise in temperature, the micellar length decreases, for both the systems while the radius of the micelles remains constant as indicated by the overlapping intensities in the high Q region. As evident, the effect is more prominent in CTAB-TYOE system compared to CTAB-TYDE system. Table 3 quantitatively summarizes the dimensions of the CTAB-aminoacid ester assemblies obtained from SANS treatment at various conditions. It may be seen that the semi major axis, a, is 4-5 times the semi-minor axis, b, in all the systems at all temperature and compositions, which confirms the cylindrical shape of the aggregates throughout. Micelles formed with TYDE as additive are nearly 40% longer than that formed in presence of TYOE (Table 3) at all temperatures. Increasing concentration of TYDE in CTAB-TYDE system from 40 to 60 mM causes an increase of ~ 20 - 40 nm in the micellar length. Increasing temperature from 303 K to 323 K decrease the micellar length by approximately 25% in each case.

Table 3. Dimension of wormlike micelles of CTAB with additives as a function of concentration and temperature obtained from SANS study.

CTAB=100mM						
Temperature (K)	TYDE 40 mM		TYDE 60 mM		TYOE 40 mM	
	Semi Major Axis (Å)	Semi Minor Axis (Å)	Semi Major Axis (Å)	Semi Minor Axis (Å)	Semi Major Axis (Å)	Semi Minor Axis (Å)
303	126.29	26.869	148.21	29.739	94.23	22.693
313	108.51	25.421	143.17	26.92	79.127	21.784
323	99.852	24.079	109.05	25.36	70.992	20.839

The SANS study corroborates the synergistic interplay between the CTAB and the aminoacid ester molecules, as observed from the study of interfacial property study, at much higher concentrations. The differences in the micellar lengths and extent of electrostatic interaction of the additives with CTAB head group arises primarily due to the difference in their molecular architecture. While both TYOE and TYDE contain identical head group, viz., the phenol ring of tyrosine moiety, the longer alkyl chain length of TYDE, viz., 12 carbon units, confers higher hydrophobicity to it compared to TYOE with 8 carbon units. Secondly, the spatial orientation of the additives and their location w.r.t CTAB monomers as well as the micelles is also likely to influence the interaction behavior of the aminoacid esters with the CTAB molecules.

3.8. End-caps and end-cap geometry

Morphology transition of cationic micelles from sphere to rod like micelles and subsequent transition to wormlike micelle via charge screening is a well studied process. Formation of rod/wormlike micelle in the present system, consisting of CTAB and TYOE or TYDE, is understood from the observation of non-Newtonian nature of flow and subsequent SANS and TEM studies. The transition from spherical to rod like micelles by tuning the surface curvature via charge screening involves topological defects at the end-caps. Such end-cap region with different curvature compared to main cylindrical body incur an added energetic penalty. This thermodynamically unfavorable situation leads to long wormlike micelles instead of large number of small rods. Therefore, among the other factors, the contour length of WLM becomes a function of end-cap energy as well. A mean field theory of the growth process of WLM for either

neutral or strongly screened system predicts the average contour length to be function of volume fraction ϕ, temperature and the end-cap energy E_C with two hemispherical end-cap model as given in the following relation:[58-60]

$$L \sim \phi^{\frac{1}{2}} \exp[{}^{E_C}/_{k_B.T}] \quad (12)$$

where k_B is the Boltzman constant.

On the other hand, a molecular level self-consistent field analysis of very long cylindrical micelles supports the idea of swollen end-caps with respect to the cylindrical part.[61] This dumbell shaped model is, however, energetically not favorable on two counts. First, in such a case, the diameter of the spheres of the dumbell shaped part be longer than twice the straight chain length of the surfactant molecule and second, the dumbell-shaped micelles contains energetically unfavorable negative curvature at the neck. Present discussion on the end-cap geometry of cylindrical micelles of CTAB is, therefore, confined to hemispherical end-caps with the possibility of perturbation on geometry due to the presence of TYOE/TYDE in the system (e.g. flat end caps).

In addition to the 2D NMR results, as shown in section 3.5.2, some further observation is also worth mentioning here. The cross peaks viz., C1-C6+T7 and C2-C6+T7 are observed and they correlate the quaternary ammonium protons of CTAB with the terminal protons of both CTAB and TYOE. C2 interacts with T7 quite obviously because of the folded structure of TYOE but interaction of C2 with C6 of the same CTAB molecule is ruled out because complete folding of CTAB molecule would lead to instability of the rod as mentioned above. Moreover, cross peaks corresponding to correlation between C3, C4 and the terminal methyl protons of CTAB are observed (indicated by elliptical symbols in Figure 7). This further indicates that the cross peaks arise from interactions of the protons from the two sets of CTAB molecules, residing at different environments. First, the NMe protons of CTAB (C1) are located close to the aromatic protons, viz., T1, T2 of TYOE facilitating cation-π interaction to take place. This orientation results in the observed cross peaks between the NMe and C1 protons with aromatic protons of TYOE. Second, from the CTAB protons residing at the end caps adjacent to the body of the rod-like micelles which exhibit the interaction between the C2, C3 protons of one CTAB molecule with the intermediate (C5) as well

as terminal protons of the other (C6) at the flat part of the cap (Figure 8 (interaction shown by elliptical symbol))

1D SCF (Self-consistent field; concentration gradient in one direction) study shows that the end-cap energy of very long wormlike micelles is nearly 2.8 k_BT per cap, which is equivalent to ~1.67 kCal.mol^{-1}.[59] Interestingly, this energy is of the order of cation-π interaction (~1.13 kCal.mol^{-1}) of the present system.

Further, lowering of the curvature of the end-caps via embedding of TYOE/TYDE in the end-cap region, just like the body of the cylinder by hydrophobic force and cation-π interaction, cannot be ruled out. Under this situation, the end-cap would suffer a perturbation on its geometry and a somewhat flat caps with positive curvature at the junction with the cylindrical body would result (Scheme 3) The CTAB and TYOE/TYDE molecules at the flat part of the cap would, therefore, direct toward the body in somewhat parallel orientation, whereas the alkyl chains of CTAB molecules of the junctions tend to converge towards the core of the micelles. The junctions with positive curvature do not accommodate TYOE/TYDE molecules and, therefore, no screening of CTAB head groups results. The molecular interactions which are present in the micelles and manifested in 2D NMR spectra are not only due to the molecules present in the cylindrical body but also for the molecules at the end-caps (shown by elliptical symbol in Scheme 3)

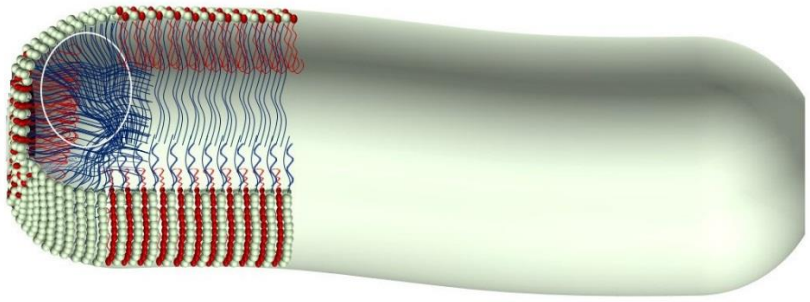

Scheme 3. Cylindrical/Worm-like micelle with flat end-caps (unusual molecular Interactions are shown by elliptical symbol

3.9. Characteristic study of rheological behavior of the CTAB-amino acid ester systems

The formation of worm-like or elongated micelles in CTAB triggered by the tyrosine analogues highly interesting, more so, because the elongated aggregates impart

viscoelastic property to the biomimetic model membrane system thereby modifying its bulk property to a huge extent. It was, therefore, tempting to study the bulk rheological property of the CTAB-aminoacid ester systems to explore its potentiality further. The concentration of CTAB (75 mM) and aminoacid esters (37 mM) i.e., at $\chi_{TYOE/TYDE}$= 0.33 was chosen as it is an intermediate between the compositions 100 mM CTAB-40 mM aminoacid ester, where $\chi_{TYOE/TYDE}$= 0.28 and CTAB (100 mM)- aminoacid ester (60 mM), where $\chi_{TYOE/TYDE}$= 0.37. The shear viscosity profile of CTAB-TYOE and CTAB-TYDE systems studied as function of temperature, show that the systems exhibit Non-Newtonian behavior at different temperature ranges (Figure 10). The shear thinning at higher shear rates may be considered as another evidence regarding presence of worm-like micelles within the system.[62]

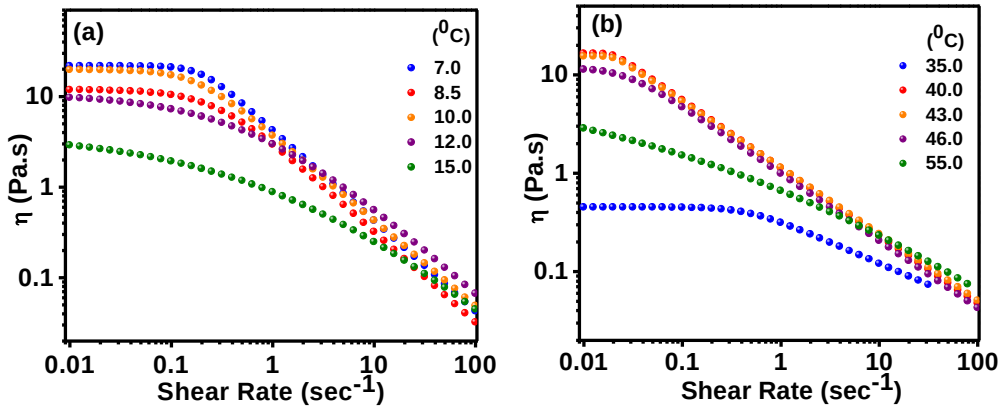

Figure 10. Shear viscosity profiles of (a) CTAB (75 mM)-TYOE (37 mM) system and (b) CTAB (75 mM)-TYDE (37 mM) system as function of temperature.

While in the case of CTAB-TYOE, the linear viscoelastic regime appeared between temperatures 7^0C and 15^0C (Figure 10 (a)), in the case of CTAB-TYDE system, the temperature range was as high as 35^0C-55^0C (Figure 10 (b)). This difference in the non-Newtonian behavior could not be explained in straightforward manner and requires more attention, which may be undertaken in a separate study. The response of the viscoelastic moduli of these model systems were examined as function of angular frequency within the observed respective viscoelastic range (Figure 11). It is evident that at shorter time scale, or high ω, elastic behavior is displayed by the samples, with storage or elastic modulus, G′, dominating over the viscous or the loss modulus, G″ (Figure 10 (a), (b)). At longer time scale, or lower ω, an opposite trend is observed, i.e., G″> G′. The dominant relaxation time,τ_R, for these CTAB-aminoacid ester systems is

estimated as $\frac{1}{\omega_C}$, where ω_C denotes the cross-over angular frequency, where G′ = G″. The observation demonstrates that the CTAB-aminoacid mixed systems behave as "living polymers" which exist in dynamic equilibrium where the micelles undergo constant breakage and recombination to form a transient network.[63] The viscoelastic response of the CTAB-TYOE and CTAB-TYDE systems is in good agreement with Maxwell's mechanical model which may be used in describing the dynamic rheological property of the present systems.[32,64]

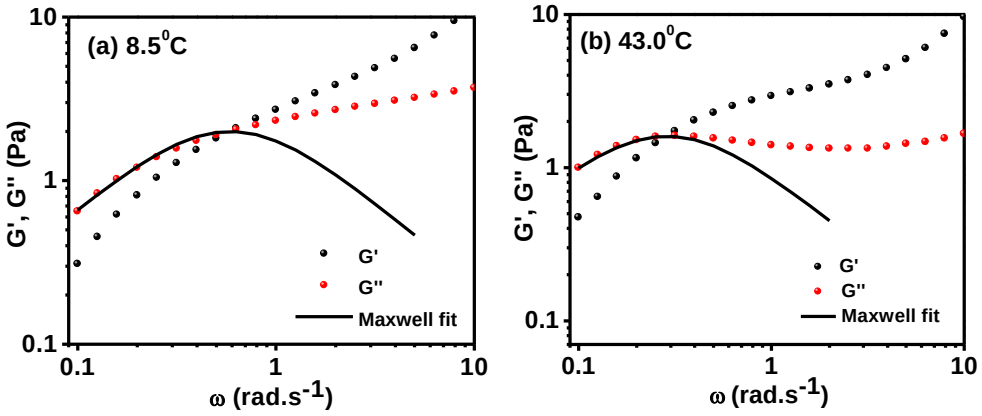

Figure 11. Representative plot of frequency sweep curves of (a) CTAB (75 mM)-TYOE (37 mM) at 8.5^{0}C, (b) CTAB (75 mM)-TYDE (37 mM) at 43.0^{0}C.

According to this model, the G′and G″ are given as-

$$G'(\omega) = G_0\omega^2\tau_R^2/(1+\omega^2\tau_R^2) \quad (12)$$

$$G''(\omega) = G_0\omega\tau_R/(1+\omega^2\tau_R^2) \quad (13)$$

where G_0 is the storage modulus at high frequency.

The oscillatory flow spectra are fitted to the theoretical curve obtained from Maxwell model (solid line in Figure 11 (a), (b)). At lower ω, the systems exhibit well-defined Maxell behavior, however at higher ω, much deviation is apparent. This deviation is caused by presence of faster modes of stress relaxation, like "Rouse or breathing modes".[55,56,48,62] From the lower values of ω_C, for CTAB-TYDE systems compared to that in CTAB-TYOE (Figure S2 of Appendix C), it may be said that the former system adopts slower reptation mode of relaxation. Slower relaxation modes may also be associated with linearity of the worm-like micelles. From the lower values of ω_C, for CTAB-TYDE systems compared to that in CTAB-TYOE (Figure S2 of Appendix C),

it may be said that the former system adopts slower reptation mode of relaxation. Slower relaxation modes may also be associated with linearity of the worm-like micelles.[65]

4. Conclusion

Synergistic improvement of the interfacial properties of the aqueous mixtures of CTAB with L-Tyrosineoctyl ester or L-Tyrosinedodecyl ester stems from cation-π interaction between quaternary ammonium head group of CTAB and π-electron cloud of aromatic aminoacid, in addition to usual non-covalent forces present in the system. The hydrophobic and hydrophilic blocks present in the molecular architecture of tyrosine analogues lead to highly folded geometry, which makes headway for unusual flipping of the molecule in the event of slight perturbation on the delicate balance of prevailing driving forces resulting in contrasting effects pertaining to hydrophobicity and micropolarity. Micellar morphology transition from cylindrical to rod/wormlike micelles via charge screening of the headgroups by π-electrons of aromatic aminoacid is indeed interesting in view of the abundance of zwitterionic phosphatidylcholine in bio-membranes and the ubiquitous feature of transmembrane proteins to localize tyrosine and tryptophan at the interface. Since the interplay between lipids and proteins is the key to how cells control membrane shape during many vital events including cellular fission, fusion and virus entry, the observed tuning of micellar surface curvature by tyrosine analogues is thought provoking and opens up avenue for new physical chemistry research on a vital biological phenomena. The end-cap geometry of the cylindrical/wormlike micelles formed via charge screening of the cationic micelles is discussed and found to be flat-cap in shape for the first time.

References are provided in BIBLIOGRAPHY under “References for Chapter VI” (Page 184-189).